Int J Clin Exp Med 2018;11(1):125-136
www.ijcem.com /ISSN:1940-5901/IJCEM0060844

Original Article

Effects of a spaceflight environment on phenotypic, genomic and transcriptomic changes in KPC-2 *Klebsiella pneumoniae*

Chou Xu[1*], Yiming Lu[2*], Yajuan Wang[1*], Xuelin Zhang[1], Hong Zhou[1], Bing Huang[1], Yi Yu[1], Jia Li[1], Changting Liu[1]

[1]Nanlou Respiratory Diseases Department, Chinese PLA General Hospital, Beijing 100853, China; [2]Beijing Institute of Radiation Medicine, Cognitive and Mental Health Research Center, State Key Laboratory of Proteomics, Beijing 100850, China. [*]Equal contributors.

Received February 12, 2017; Accepted December 15, 2017; Epub January 15, 2018; Published January 30, 2018

Abstract: As a highly drug-resistant and widely spread pathogen, carbapenemase (KPC)-producing *Klebsiella pneumoniae* represents an urgent public health crisis. Variations in the ability to cope with environmental hazards increase a microbe's survival chances. Therefore, understanding such adaptive mechanisms will be beneficial for controlling the spread *K. pneumoniae* and the development of anti-infective therapies. The extreme environment in spaceflight represents a unique research platform. We compared phenotypic variations and analyzed genomic and transcriptomic variations in KPC-2 *K. pneumoniae* among three different groups: strains T (15 days of Shenzhou X spaceflight), D (the ground control) and F (the reference strain). We found no obvious variations in the drug susceptibility, carbon source utilization, biofilm-forming capacity, and shapes and arrangements of bacterial cells of the D and T strains; however, the growth rates and final concentrations of the bacterial cells decreased when cultured in hypertonic LB medium (8% sodium chloride). Additionally, high-throughput sequencing revealed some genomic mutations and differentially regulated transcriptomes between the D and T strains. These results provide insights into the environmental adaptation of this widespread pathogen.

Keywords: Spaceflight, phenotype, genome, transcriptome, *Klebsiella pneumonia*

Introduction

Space environments are associated with a variety of special stressors, such as low gravity, strong radiation, and weak magnetic fields, that can accelerate the microbial mutation rate and introduce more varied mutations [1]. Previous space studies on pathogens have mostly focused on mutations that produce changes in drug resistance. After the initial studies from Space Station Salyut 7 [2], many bacteria have been reported to exhibit changes in drug resistance after spaceflight [3, 4]. We previously reported that by obtaining an extra copy of the *sul1* gene, a strain of *Klebsiella pneumoniae* gained resistance to cotrimoxazole after being carried by the Shenzhou VIII spacecraft [5]. In addition, *Bacillus cereus* became resistant to ceftazidime due to changes in its transcriptome and proteome [6], whereas New Delhi metallo-β-lactamase 1 (NDM-1)-producing *K. pneumoniae* carried by the Shenzhou X spacecraft maintained its resistance [7]. The influences of a space environment on bacteria are multidimensional; spaceflight can cause a 'stimulating effect' on microbial growth [8-10] and even microbial secondary metabolism [11]. We also found phenotypic, genomic, transcriptomic and proteomic changes in many pathogens, including *Staphylococcus aureus* [12], *B. cereus* [6], *Serratia marcescens* [13], *Enterococcus faecium* [14], *Escherichia coli* [15] and NDM-1 *K. pneumoniae* [7]. Accordingly, some mutations that rarely occur on the ground can be induced and amplified by the special physical and chemical environmental factors in space. These alterations in microorganisms will not only jeopardize astronauts but also threaten people on Earth [16]. Therefore, revealing mutations that occur in space provides an unprecedented plat-

form and possibility for understanding pathogens.

K. pneumoniae, which is a common opportunistic human pathogen, causes a wide range of hospital- and community-acquired infections. Among the highly drug resistant and rapidly spreading *K. pneumoniae* strains, *K. pneumoniae* carbapenemase (KPC)-producing strains represent the highest proportion and are responsible for an unprecedented public health crisis [17]. KPC-2 is one of the most prevalent isoenzymes among the KPCs according to many clinical surveys [18-20]. The successful persistence and dispersion techniques used by highly drug-resistant bacteria remain largely unknown but may be partially dependent on their superb adaptation to harsh environments. Thus, understanding the ability of this pathogen to cope with hostile environments and various stressors could facilitate our comprehension of its pathobiology. Additionally, identifying genomic and transcriptomic variations caused by environmental adaptation will contribute to the development of methods to control its persistence and spread. The Shenzhou X spacecraft was launched on June 11, 2013, and flew in space for 15 days; this spacecraft provided a unique extreme environment to explore the adaptation of this pathogen.

In this study, KPC-2 *K. pneumoniae* strain ATCC BAA-1705 (F strain) was cultured in semisolid Luria-Bertani (LB) medium in the Shenzhou X spacecraft (T strain) and on the ground statically (D strain) for 15 days. Both groups were cultured in the same medium volume at the same initial concentration. After spaceflight, we performed phenotypic analyses and comparative genomic and transcriptomic analyses to explore the impact of the extreme environmental conditions encountered in spaceflight on this pathogen.

Materials and methods

Bacterial strains and culture conditions

The reference strain *K. pneumoniae* ATCC BAA-1705 (F strain) was used in the study. The bacterium was cultivated in semisolid LB medium (10 g/L of tryptone, 5 g/L of yeast extract, 10 g/L of NaCl, and 5 g/L of low-melting-point agar) in the Shenzhou X spacecraft (T strain) and on the ground (D strain). Both the D and T strains were grown in an airtight tube at 21°C for 15 days. For the phenotypic analysis, the strains were cultured in LB medium. Growth curves of the strains were monitored at 600 nm in a Bioscreen C microbial growth curve analysis system (Oy Growth Curves Ab Ltd., Raisio, Finland) at 37°C.

Drug susceptibility testing

Drug susceptibility testing and the minimum inhibitory concentrations (MICs) of ampicillin, ampicillin/sulbactam, piperacillin/tazobactam, cefazolin, cefotetan, ceftazidime, ceftriaxone, cefepime, aztreonam, ertapenem, imipenem, amikacin, gentamicin, tobramycin, ciprofloxacin, levofloxacin, furadantin, and trimethoprim-sulfamethoxazole against the *K. pneumoniae* strains were assessed using the VITEK-2 COMPACT automated microbiology system (BioMérieux, France) following the manufacturer's instructions. The results were interpreted according to the Clinical and Laboratory Standards Institute (CLSI) guidelines. *E. coli* strain ATCC 25922 was used as a quality control for the drug susceptibility testing.

Carbon source utilization assays and chemical sensitivity assays

The *K. pneumoniae* strains were cultured overnight and then inoculated into IF-A inoculating fluid (Biolog, CA, USA). The target bacterial density in the inoculating fluid was adjusted to 90-98% T using a turbidimeter. Then, 100 μL of culture was added to each well of the Biolog GEN III MicroPlate (Biolog, CA, USA). After incubating for 24 hours at 37°C, the absorbance of each testing well was measured with a BIOLOG microplate reader at 590 nm and confirmed visually against the control wells.

Biofilm formation assay

Each *K. pneumoniae* strain was cultured overnight, diluted 100-fold in LB medium and then inoculated into 96-well polystyrene microtiter plates. After static incubation for 36 h at 37°C, the wells were washed 3 times with phosphate-buffered saline (PBS, pH 7.4). After fixation in methanol and air drying, the attached cells were stained with crystal violet (1% w/v; Sigma). Then, the wells were washed to remove excess

Table 1. Drug resistance profiles of the *K. pneumoniae* strains

Antimicrobial category	Drugs*	MIC (μg/mL)		
		F	D	T
Penicillins	AMP	≥32	≥32	≥32
Penicillins + beta-lactamase inhibitors	SAM	≥32	≥32	≥32
Antipseudomonal penicillins + beta-lactamase inhibitors	TZP	≥128	≥128	≥128
1st and 2nd generation cephalosporins	CFZ	≥64	≥64	≥64
Cephamycins	CTT	32	32	32
3rd and 4th generation cephalosporins	CAZ	≥64	≥64	≥64
	CRO	≥64	≥64	≥64
	FEP	8	8	8
Monobactams	ATM	≥64	≥64	≥64
Carbapenems	ETP	≥8	≥8	≥8
	IMP	4	4	4
Fluoroquinolones	AMK	≥64	≥64	≥64
	GM	4	2	4
	TOB	≥16	≥16	≥16
Fluoroquinolones	CIP	≥4	≥4	≥4
	LVX	≥8	≥8	≥8
Nitrofurantoin	FD	≥512	≥512	≥512
Folate pathway inhibitors	SXT	≥320	≥320	≥320

*Abbreviations: AMP, Ampicillin; SAM, Ampicillin/Sulbactam; TZP, Piperacillin/Tazobactam; CFZ, Cefazolin; CTT, Cefotetan; CAZ, Ceftazidime; CRO, Ceftriaxone; FEP, Cefepime; ATM, Aztreonam; ETP, Ertapenem; IMP, Imipenem; AMK, Amikacin; GM, Gentamycin; TOB, Tobramycin; CIP, Ciprofloxacin; LVX, Levofloxacin; FD, Furadantin; SXT, Trimethoprim-Sulfamethoxazole.

crystal violet and air dried. After solubilization in 33% (w/v) acetic acid, the absorbance of the stained biomass in each well was measured at 590 nm. The biofilm formation assay results were adjusted based on the cell concentration. All experiments were repeated at least three times.

Scanning electron microscopy (SEM)

After growth in LB medium overnight, the bacterial cells were washed with sterile PBS (pH 7.4), resuspended in 2.5% (v/v) glutaraldehyde solution in 0.1 M PBS, and fixed overnight at 4°C. The fixed cells were rinsed three times with PBS to remove glutaraldehyde and post-fixed in 1% osmium tetroxide solution. After 1 h, the cells were washed three times with PBS and dehydrated in a graded ethanol series (30%, 50%, 70%, 85%, 95%, 100%, and 100%, each for 15 min). For SEM assay, cells were washed with isoamyl acetate, critical point dried, coated with gold/palladium, and observed and photographed under a scanning electron microscope (Hitachi S-3400N, Tokyo, Japan).

Genome sequencing

Genome sequencing was performed by the Beijing Genomics Institute (BGI, China). Genomic DNA was extracted from each strain using the conventional phenol-chloroform method. After purification, a 100 × 500-bp paired-end library was constructed for each DNA sample. Standard Illumina paired-end reads 500-bp in length were generated for the strains on the Illumina Hiseq 2000 sequencing platform with 90 cycles. Low-quality sequence reads were filtered using the DynamicTrim and LengthSort Perl scripts within SolexaQA. Short reads were assembled using SOAPdenovo (http://soap.genomics.org.cn/soapdenovo.html, version: 2.04).

Genetic variant identification and phylogenetic analysis

To evaluate genomic variants, we identified strain-specific single nucleotide polymorphisms (SNPs) by aligning the reads of the D or T strain to the F strain using the SOAP2 program and SOAPsnp [21, 22]. The SOAPsnp results were filtered by removing low-quality reads (sequences were trimmed with a quality score ≤Q20); trimmed reads with fewer than 30 bp were ignored. All SNPs were called and mapped to the F strain and assigned coordinates.

Transcriptome sequencing and comparative transcriptomic data analysis

Total RNA was extracted from the F, D and T strains using the RNeasy Protect Bacteria Mini Kit (QIAGEN, Germany) according to standard-

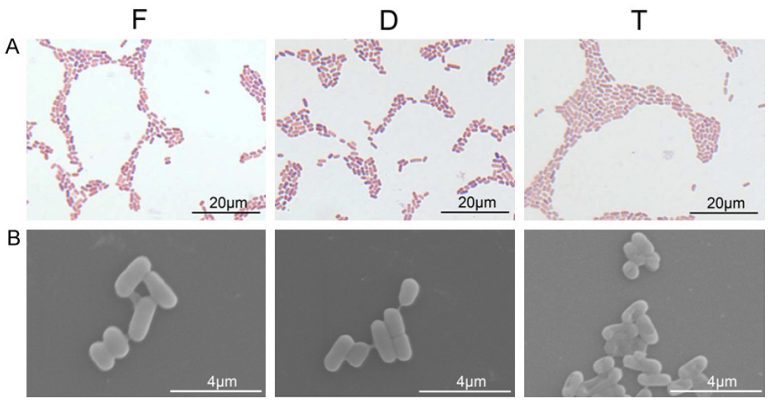

Figure 1. Morphology of the *K. pneumoniae* strains. A. Hematoxylin and eosin staining of the *K. pneumoniae* strains (magnification × 1000). B. Scanning electron micrographs of the *K. pneumoniae* strains.

ized protocols. cDNA libraries were constructed for the three strains and sequenced by BGI (China). After quantification and qualification, the libraries were sequenced using the Illumina Hiseq 2500 platform by running 90 cycles to generate paired-end sequences. In the quality-control step, clean data (clean reads) were obtained by removing reads containing adapters and poly-N and low-quality reads from the raw data. The reference genome index was built using Bowtie2 (v2.2.3) [23], and paired-end clean reads were aligned to the reference genome using TopHat (v2.0.9) [24] L. HTSeq (v0.6.1) was used to count the read numbers mapped to each gene. Additionally, the RPKM (Reads Per Kilobase of exon model per Million mapped reads) of each gene was calculated based on the length of the gene and the read counts mapped to the target gene [25]. A differential expression analysis was performed using the edgeR package. The *p*-values were adjusted using the Benjamini and Hochberg method. An adjusted *p*-value of 0.001 and log2 (fold change) of 1 were set as the thresholds for significant differential expression. Finally, functional enrichment analyses of differentially expressed genes (DEGs) were implemented using the BLASTALL software against the Cluster of Orthologous Groups (COG) database.

Statistical analysis.

Differences in biofilm-forming capacities among the three strains were performed using one-way analysis of variance (ANOVA), and the data were analyzed using the statistical computer software SPSS 20.0 (SPSS Inc., Chicago, IL, USA). Two-way ANOVA was applied to analyze bacterial growth curves, and the analysis was performed by GraphPad Prism 5 (GraphPad Software, Inc., La Jolla, CA, USA). A *p*-value less than 0.05 was considered to be statistically significant.

Results

Phenotypic characteristics of the K. pneumoniae strains

Based on multilocus sequence typing (MLST), *K. pneumoniae* ATCC BAA-1705 (F strain) belongs to sequence type 258 (ST258). The drug susceptibility testing results showed that the F strain was resistant to most of the tested drugs with the exception of cefepime (MIC=8 μg/mL) and gentamicin (MIC=4 μg/mL). The D and T strains showed no significant changes compared with the F strain (**Table 1**). When examined using light microscopy and SEM, no obvious changes were observed in the morphological shapes and arrangements of bacterial cells among the three strains (**Figure 1**). The fitness of the *K. pneumoniae* strains was assessed by determining the growth rates in standard LB and hypertonic LB media (4% and 8% sodium chloride, respectively). Both the D and T strains had growth curves that were similar to the F strain in the standard LB medium and 4% sodium chloride LB medium (**Figure 2A**, **2B**). In the hypertonic LB medium with 8% sodium chloride, all three strains exhibited prolonged lag phases and shorter logarithmic and stationary phases. The hypertonic medium reduced the growth rate and the final population density of this pathogen. However, in the 8% sodium chloride LB medium, the growth rate and final concentration of the bacterial cells decreased in the following sequence: F strain > D strain > T strain (**Figure 2C**).

The ability to form biofilms is thought to be related to adaptability to environmental persistence and is an important phenotype for drug resistance and host colonization [26, 27]. After spaceflight, NDM-1 *K. pneumoniae* exhibited an increased ability to form biofilms [7], whereas the D and T strains showed biofilm-forming capacities similar to the F strain after incuba-

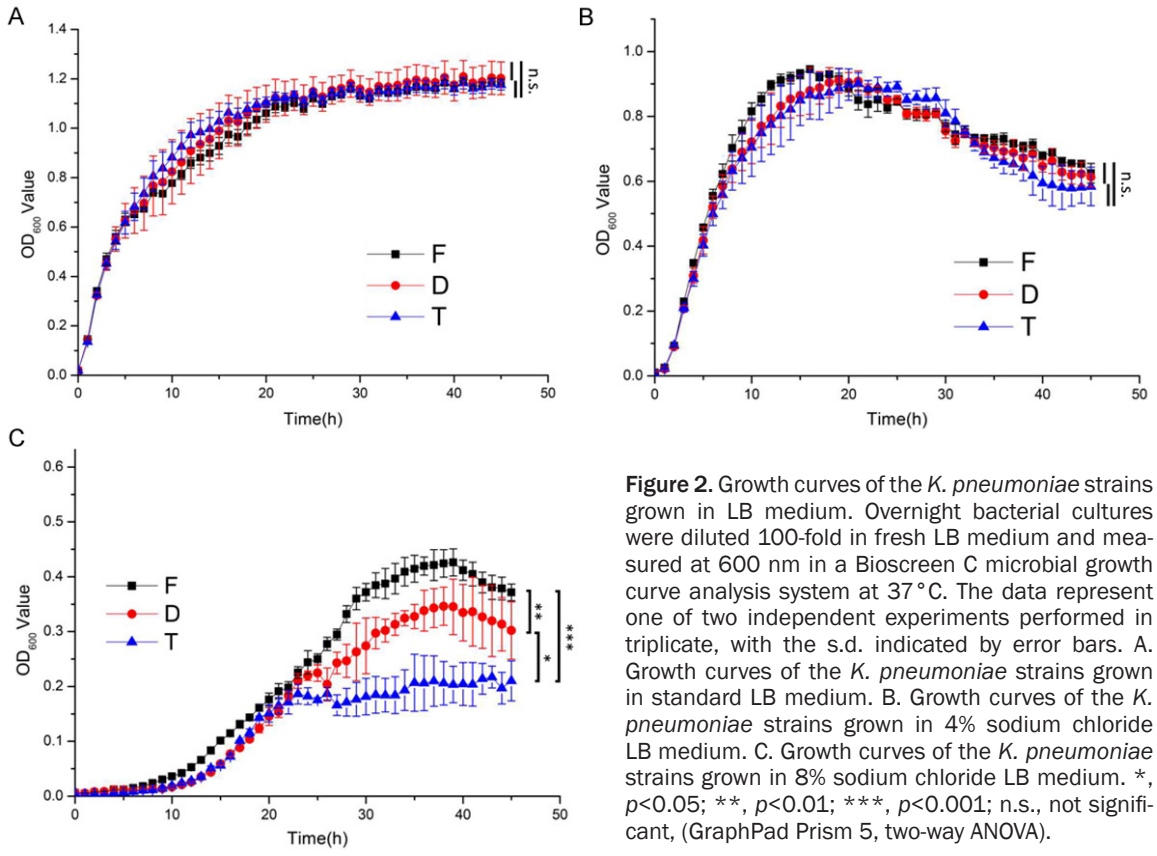

Figure 2. Growth curves of the *K. pneumoniae* strains grown in LB medium. Overnight bacterial cultures were diluted 100-fold in fresh LB medium and measured at 600 nm in a Bioscreen C microbial growth curve analysis system at 37°C. The data represent one of two independent experiments performed in triplicate, with the s.d. indicated by error bars. A. Growth curves of the *K. pneumoniae* strains grown in standard LB medium. B. Growth curves of the *K. pneumoniae* strains grown in 4% sodium chloride LB medium. C. Growth curves of the *K. pneumoniae* strains grown in 8% sodium chloride LB medium. *, $p<0.05$; **, $p<0.01$; ***, $p<0.001$; n.s., not significant, (GraphPad Prism 5, two-way ANOVA).

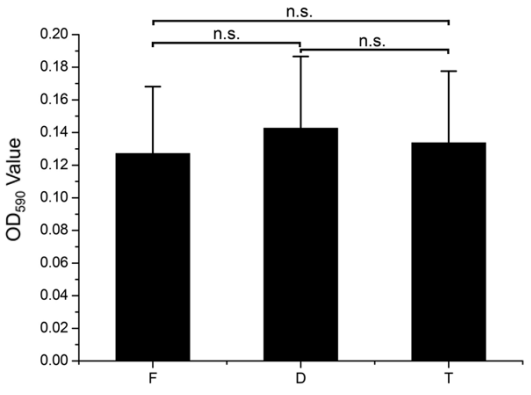

Figure 3. Biofilm formation ability of the *K. pneumoniae* strains. The absorbance of the biofilm stained with crystal violet was measured at 590 nm for each strain. The amount of biofilm was controlled by the cell concentration. By one-way ANOVA using SPSS statistical software version 20.0 (SPSS Inc., Chicago, IL, USA), there were no significant differences among the three strains ($p=0.824$). n.s., not significant.

tion for 36 h at 37°C (**Figure 3**). We also evaluated carbon source utilization and performed a chemical sensitivity assay using 96-well Biolog GEN III MicroPlates. The results from 71 carbon source utilization assays and 23 chemical sensitivity assays showed that the D and T strains exhibited no obvious changes compared to the F strain (**Table 2**).

Whole genome sequencing analysis of mutations in the D and T strains compared with the F strain

The whole genome sequencing results from the D and T strains are presented in **Table 3**. The read mapping results reported nearly complete genome coverage (> 99.99%) for the D and T strains. No large insertions and deletions (InDels) were found in these two strains compared to the F strain. A total of 90 and 84 mutations were identified in the D and T strains, respectively, and 75 mutations were found in both strains (**Figure 4A**). In total, 22 mutations in coding sequences (CDSs) were identified in the D and T strains (**Table 4**), including seven specific mutations in the D strain, two specific mutations in the T strain and 13 mutations shared by the two strains (**Figure 4B**). Seven SNPs were associated with the conjugal/conjugal transfer pilus assembly protein.

Table 2. Carbon source utilization patterns and chemical sensitivity of the *K. pneumoniae* strains. "+" represents a positive reaction; "-" represents a negative reaction

	Carbon sources/Chemicals	F	D	T
A1	Negative Control	-	-	-
A10	Positive Control	+	+	+
Carbon source utilization patterns				
A2	Dextrin	-	-	-
A3	D-Maltose	-	-	-
A4	D-Trehalose	-	-	-
A5	D-Cellobiose	+	+	+
A6	Gentiobiose	+	+	+
A7	Sucrose	+	+	+
A8	D-Turanose	-	-	-
A9	Stachyose	+	+	+
B1	D-Raffinose	+	+	+
B2	α-D-Lactose	+	+	+
B3	D-Melibiose	+	+	+
B4	β-Methyl-D-Glucoside	+	+	+
B5	D-Salicin	-	-	-
B6	N-Acetyl-D-Glucosamine	+	+	+
B7	N-Acetyl-β-D-Mannosamine	-	-	-
B8	N-Acetyl-D-Galactosamine	-	-	-
B9	N-Acetyl Neuraminic Acid	-	-	-
C1	α-D-Glucose	+	+	+
C2	D-Mannose	+	+	+
C3	D-Fructose	+	+	+
C4	D-Galactose	-	-	-
C5	3-Methyl Glucose	-	-	-
C6	D-Fucose	-	-	-
C7	L-Fucose	+	+	+
C8	L-Rhamnose	-	-	-
C9	Inosine	+	+	+
D1	D-Sorbitol	+	+	+
D2	D-Mannitol	+	+	+
D3	D-Arabitol	-	-	-
D4	myo-Inositol	+	+	+
D5	Glycerol	-	-	-
D6	D-Glucose-6-PO4	+	+	+
D7	D-Fructose-6-PO4	+	+	+
D8	D-Aspartic Acid	-	-	-
D9	D-Serine	-	-	-
E1	Gelatin	-	-	-
E2	Glycyl-L-Proline	-	-	-
E3	L-Alanine	-	-	-
E4	L-Arginine	-	-	-
E5	L-Aspartic Acid	-	-	-
E6	L-Glutamic Acid	-	-	-
E7	L-Histidine	-	-	-
E8	L-Pyroglutamic Acid	-	-	-
E9	L-Serine	-	-	-
F1	Pectin	-	-	-
F2	D-Galacturonic Acid	+	+	+
F3	L-Galactonic Acid Lactone	+	+	+
F4	D-Gluconic Acid	+	+	+
F5	D-Glucuronic Acid	+	+	+
F6	Glucuronamide	+	+	+
F7	Mucic Acid	+	+	+
F8	Quinic Acid	-	-	-
F9	D-Saccharic Acid	-	-	-
G1	p-Hydroxy-Phenylacetic Acid	-	-	-
G2	Methyl Pyruvate	-	-	-
G3	D-Lactic Acid Methyl Ester	-	-	-
G4	L-Lactic Acid	-	-	-
G5	Citric Acid	-	-	-
G6	α-Keto-Glutaric Acid	-	-	-
G7	D-Malic Acid	-	-	-
G8	L-Malic Acid	-	-	-
G9	Bromo-Succinic Acid	-	-	-
H1	Tween 40	-	-	-
H2	γ-Amino-Butryric Acid	-	-	-
H3	α-Hydroxy-Butyric Acid	-	-	-
H4	β-Hydroxy-D,L-Butyric Acid	-	-	-
H5	α-Keto-Butyric Acid	-	-	-
H6	Acetoacetic Acid	-	-	-
H7	Propionic Acid	-	-	-
H8	Acetic Acid	-	-	-
H9	Formic Acid	-	-	-
Chemical sensitivity				
A11	pH 6	+	+	+
A12	pH 5	+	+	+
B10	1% NaCl	+	+	+
B11	4% NaCl	+	+	+
B12	8% NaCl	+	+	+
C10	1% Sodium Lactate	+	+	+
C11	Fusidic Acid	+	+	+
C12	D-Serine	+	+	+
D10	Troleandomycin	+	+	+
D11	Rifamycin SV	+	+	+
D12	Minocycline	+	+	+
E10	Lincomycin	+	+	+
E11	Guanidine HCl	+	+	+
E12	Niaproof 4	+	+	+
F10	Vancomycin	+	+	+
F11	Tetrazolium Violet	+	+	+
F12	Tetrazolium Blue	+	+	+
G10	Nalidixic Acid	+	+	+
G11	Lithium Chloride	+	+	+
G12	Potassium Tellurite	+	+	+
H10	Aztreonam	+	+	+
H11	Sodium Butyrate	+	+	+
H12	Sodium Bromate	-	-	-

Table 3. Statistics of whole-genome sequencing of the D and T strains

Sample	D strain	T strain
Sequencing depth (x)	124	124
Genome coverage (%)	99.99	100
Chromosome size (bp)	5,668,104	5,667,661
No. of scaffolds	97	96
No. of contigs	122	109
Largest scaffold length (bp)	674,998	675,009
N50 scaffold length (bp)	237,476	237,685
G + C content (%)	57.14	57.14
No. of genes	5600	5603
Total gene length (bp)	4,947,807	4,945,833
Average gene length (bp)	884	883
Genome coding percentage (%)	87.14	87.11

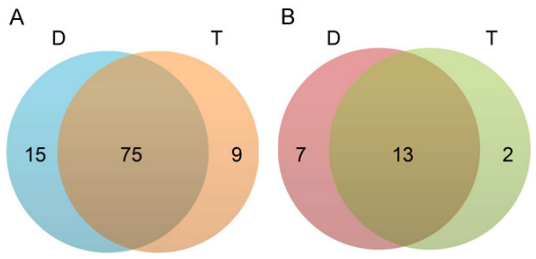

Figure 4. The number of mutations in the D and T strains compared with the F strain. A. The number of mutations in the D and T strains. B. The number of mutations in the CDSs of the D and T strains.

RNA-seq mapping and comparative transcriptomic analysis

The summary of RNA sequencing data is presented in **Table 5**. The D and T strains contained significantly more up-regulated than down-regulated genes (**Figure 5A**, **5B**). The expression patterns of DEGs identified among the D, T and F strains (fold changes > 2) are shown in **Figure 5C**. The D strain contained 132 up-regulated and 9 down-regulated DEGs and the T strain contained 482 up-regulated and 30 down-regulated DEGs compared to the F strain (**Figure 5D**). The DEGs were classified based on COG enrichment analysis (**Figure 6**). The up-regulated DEGs in the D and T strains were involved in inorganic ion transport and metabolism, amino acid transport and metabolism, and carbohydrate transport and metabolism, whereas the up-regulated DEGs from the T strain were also involved in transcription. The T strain contained 28 up-regulated and 2 down-regulated DEGs compared to the D strain (**Figure 5D**), which were characterized by the regulation of genes involved in general functions, coenzyme transport and metabolism and carbohydrate transport and metabolism.

Discussion

The worldwide emergence and dissemination of highly drug-resistant bacterial pathogens, such as KPC-2 *K. pneumoniae*, pose a considerable threat to public health. In general, the hazards of pathogenicity in bacteria are caused not only by their high drug resistance but also by their tenacious vitality, flexible adaptation and persistence [28]. Therefore, understanding the formidable strategies used by pathogens to cope with complex and volatile environments is one of the multitier approaches for the assessment and prevention of the threat. We adopted an approach investigating phenotypic, genomic and transcriptomic variations to gain new insights into the pathogen's success as a "superbug".

Spaceflight is a unique stress that drives evolution and adaptation. Thus, spaceflight is a model system for studies of many evolutionary and adaptation questions about pathogens. *K. pneumoniae* ATCC BAA-1705 (T strain), which was grown in the Shenzhou X spacecraft for 15 days, had to cope with overload acceleration, microgravity, space radiation, and growth in a defined medium with metabolite accumulation and limited nutrients. In this study, we compared differences between three *K. pneumoniae* strains. The comparison of the D and F strains indicates the effects of special culture methods, the comparison of the D and T strains indicates spaceflight effects, and the comparison of the T and F strains indicates both the influence of spaceflight and the effects of special culture methods.

The D and T strains exhibited a drug resistance phenotype that was similar to the F strain, suggesting that KPC-2 *K. pneumoniae* ST258 did not change its multidrug resistance phenotype or lose drug resistance-associated genes after 15 days under extremely harsh conditions. We speculate that the tenacious vitality and the not easily lost drug resistance phenotype may contribute to global success above and beyond the highly transmissible nature of KPC-2 *K. pneumoniae*. KPC-2 *K. pneumonia* showed excellent

Table 4. Summary of all SNPs identified in the CDS of D and T strains

Strain	Mutation position	Gene name	Product	Start	End	Feature interval length	Product length
D and T	G282801A	KPBAA1705_06381	Tyrosine autokinase	281,190	283,346	2157	718
D and T	T61006A	KPBAA1705_13790	6-phosphogluconate phosphatase	60,915	61,580	666	221
D and T	T43760C/C43931A/C43966T	KPBAA1705_25754	Putative dehydrogenase	43,482	44,384	903	300
D and T	C264T	KPBAA1705_26834	Hypothetical protein	1	650	650	216
D and T	C729T/C732G	KPBAA1705_27289	Conjugal transfer nickase/helicase TraI	1	881	881	294
D and T	T177C/C282A	KPBAA1705_27692	Conjugal transfer pilus assembly protein TraU	63	596	534	177
D and T	A489G	KPBAA1705_27942	Conjugal transfer ATP-binding protein TraC	1	671	671	224
D and T	A1197G	KPBAA1705_28017	Conjugal transfer pilus assembly protein TraH	1	1281	1281	426
D and T	A279C	KPBAA1705_28042	Conjugal transfer nickase/helicase TraI	1	569	569	190
D	A162691C	KPBAA1705_12654	Hypothetical protein	161,880	162,791	912	303
D	A23695C	KPBAA1705_26224	Putative oxidoreductase	23,011	24,018	1008	335
D	G119A	KPBAA1705_26834	Hypothetical protein	1	650	650	216
D	T448C/A457G/T535G	KPBAA1705_27527	Conjugal pilus assembly protein TraF	23	622	600	199
D	G818A	KPBAA1705_28017	Conjugal transfer pilus assembly protein TraH	1	1281	1281	426
T	A168295C	KPBAA1705_05931	Sugar efflux transporter B	168,198	169,379	1182	393
T	T63952G	KPBAA1705_09853	Transcriptional regulator yeeY	63,137	64,039	903	300

Table 5. Summary of RNA sequencing data

Sample	F	D	T
Raw Reads Number	16,245,638	15,997,542	14,157,560
Raw Bases Number	1,624,563,800	1,599,754,200	1,415,756,000
Clean Reads Number	15,436,842	15,095,952	13,551,476
Clean Reads Rate (%)	95.02	94.36	95.72
Clean Bases Number	1,543,684,200	1,509,595,200	1,355,147,600
Low-quality Reads Number	231,142	240,408	201,328
Low-quality Reads Rate (%)	1.42	1.5	1.42
Adapter-polluted Reads Number	376,514	465,160	230,052
Adapter-polluted Reads Rate (%)	2.32	2.91	1.62
Raw Q30 Bases Rate (%)	91.85	91.35	92.45
Clean Q30 Bases Rate (%)	93.19	92.91	93.55
Ns Reads Number	115,032	102,010	98,270
Ns Reads Rate (%)	0.71	0.64	0.69
rRNA Mapping Ratio (%)	0.53	0.59	0.54

vitality and regenerative abilities under high osmotic pressure and in high-salt medium (8% sodium chloride). In the presence of an increased sodium chloride concentration, KPC-2 *K. pneumonia* lowered its growth rate and population density. We speculate that this approach is a persistence strategy against hyperosmotic stress for bacteria and may be the same strategy used by bacteria against sublethal drug treatment [28]. Although the three strains showed similar growth curves in common LB medium, we unexpectedly discovered that the D and T strains lowered their growth rates compared with the ancestor (F strain) when cultured in hypertonic LB medium with 8% sodium chloride, especially the T strain. We speculate that KPC-2 *K. pneumoniae* more easily enters the bacterial persistence stage through adaptation and natural selection under stress after spaceflight and culture for 15 days in defined and nutrient limited environments; this survival strategy is also employed by bacteria to overcome environmental hazards. KPC-2 *K. pneumoniae* did not change its morphological shape, arrangement, ability to form biofilms, ability to utilize carbon sources and chemical sensitivity after spaceflight, which was in contrast to the results obtained for NDM-1 *K. pneumoniae* carried by the Shenzhou X spacecraft [7]. These phenomena suggest that different species have different strategies to cope with the same extreme spaceflight environment.

Bacterial genomic variation is thought to be an adaptation strategy to a specific living environment or a result of "environmental selection".

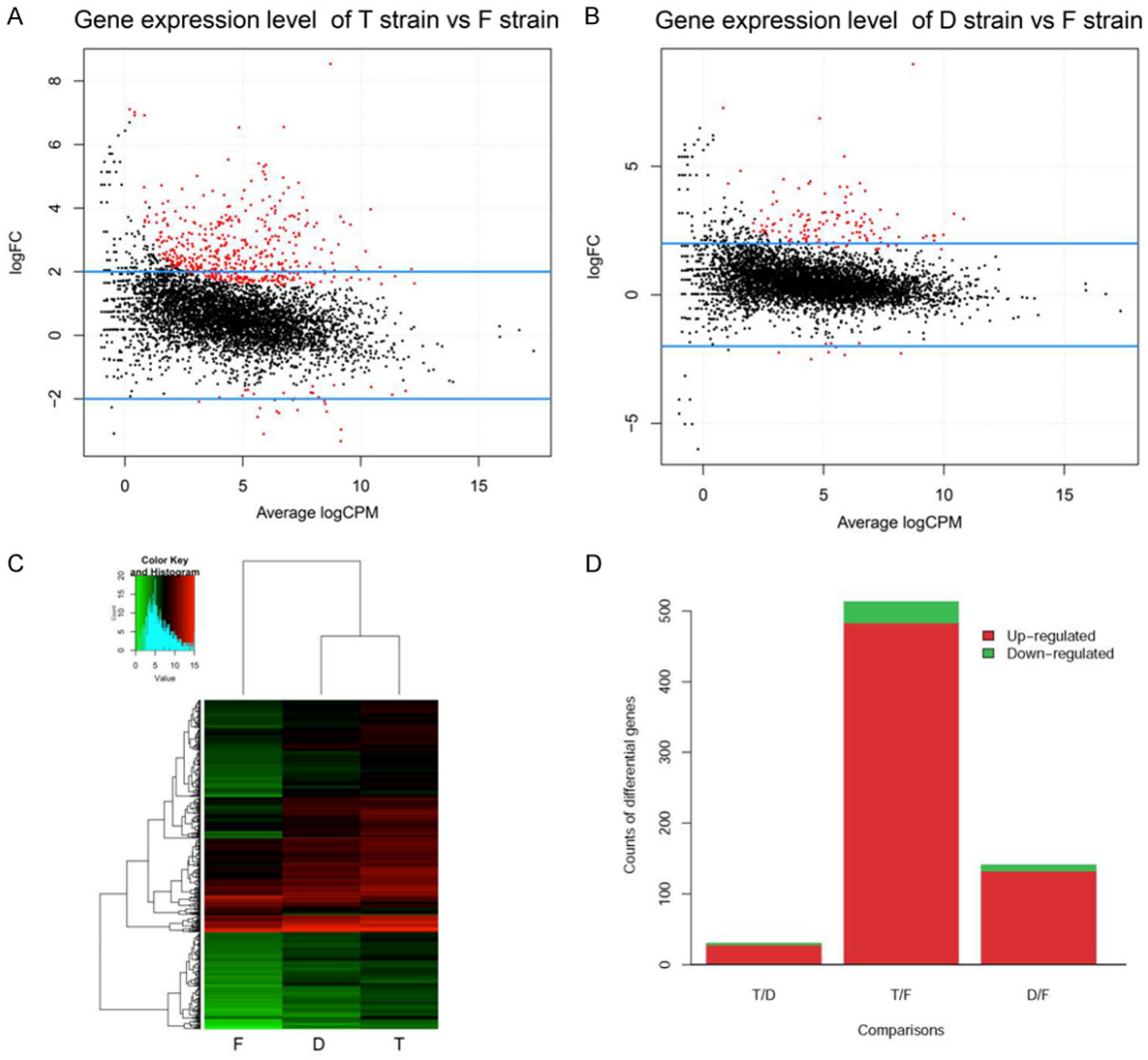

Figure 5. Statistical analysis of the number of regulated genes. A, B. Global profiling of gene-expression changes in the T vs F strain and D vs F strain comparisons. The DEGs are shown in red. C. Expression of DEGs identified among the F, D and T strains (fold changes > 2). The heatmap was generated from a hierarchical cluster analysis of genes. The RPKM values were mean-centered and normalized across samples, with each row representing a different gene. D. The number of DEGs (fold changes > 2) shown by the D (D/F) and T strains (T/F) compared to the F strain and the T strain compared to the D strain (T/D).

The genomic variants identified in this study could provide important clues to the mechanisms underlying bacterial sensing and responses to environmental stresses. Due to the conserved characteristics of CDSs, only a small fraction of mutations is located in these regions. Our results showed that seven SNPs were associated with the conjugal/conjugal transfer pilus assembly protein, which indicated that the conjugal pilus was more easily affected under stress. Additionally, many mutations were shared by the D and T strains, which was similar to the results obtained for the NDM-1 *K. pneumoniae* strain carried by the Shenzhou X spacecraft [7]. Because the KPC-2 *K. pneumoniae* strains were cultured using the same method reported for NDM-1 *K. pneumoniae*, we speculated that all strains underwent adaptive genomic variation to cope with the metabolite accumulation and limited nutrient availability. The specific mutations between the D and T strains might be the result of exposure to different combination of stressors, such as those encountered during spaceflight.

The comparative transcriptomic analysis resulted in hundreds of DEGs in the D/F and T/F comparisons. The two comparisons showed that

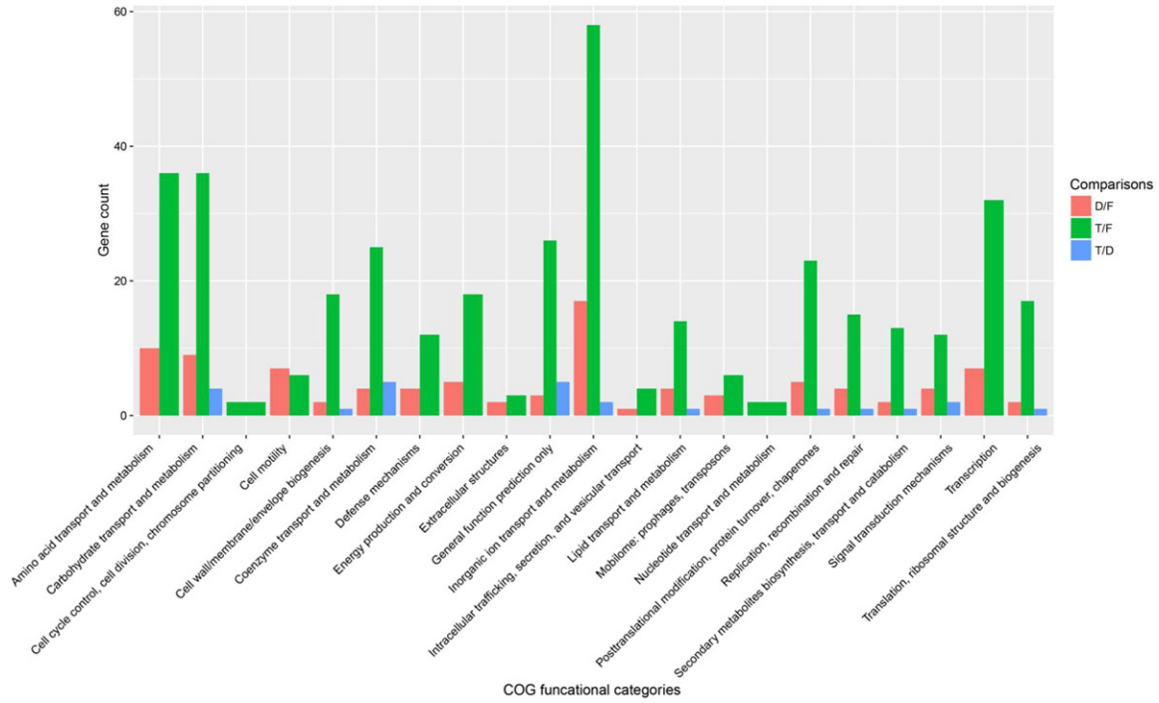

Figure 6. Distribution of DEGs among the COG functional categories. The y-axis represents the number of genes in each COG category.

more DEGs were up-regulated than down-regulated. The DEGs in D/F illustrated that living in a limited nutrient environment for 15 days significantly affected the bacterial gene expression profiles. However, the number of DEGs in T/F was greater than the number in D/F. This phenomenon revealed that the gene expression profile of the T strain was more dysregulated (mostly up-regulated) after 15 days of spaceflight due to the severe space environment. According to the COG database, DEGs regulating the transport and metabolism of inorganic ions, amino acids and carbohydrates were up-regulated in the D and T strains. These results suggest that the KPC-2 strain is a highly drug-resistant pathogenic bacterial strain with good flexibility that can adapt to stress conditions (i.e., in response to nutrient limitation and metabolite accumulation) by regulating multiple physiological processes. Additionally, some DEGs were identified in the T/D comparison, which was consistent with the increased stress during spaceflight. The top two COG categories in the T/D comparison were coenzyme transport and metabolism and carbohydrate transport and metabolism, which was consistent with our previous report investigating the NDM-1 *K. pneumoniae* strain [7]. Consistent with a previous report of *E. coli* in space [29], several genes associated with thiamine biosynthesis were up-regulated in the T/F comparison (data not shown). Synthesis of thiamine is required for carbohydrate metabolism, and *E. coli* increases production of thiamine in response to "starvation conditions" [30, 31]. These similar variations represent useful information for further studies of bacterial adaptability in spaceflight.

To date, few studies have investigated the effects of osmotic stress on *K. pneumoniae*. In this study, we found that some of the DEGs in the T/F and D/F comparisons were associated with osmotic pressure-compatible solutes, such as fucose, proline, glutamine, and sodium transporters [32]. These DEGs probably have some relationship with the different growth curves in the high-osmotic medium. Because adaptation to hyperosmotic stress is an important survival strategy for pathogens, these results need to be pursued further.

In conclusion, using phenotypic characteristics and high-throughput sequencing analysis, we found that KPC-2 *K. pneumoniae* significantly changed its phenotype, genome and transcrip-

tome after 15 days of spaceflight compared to bacteria cultured on the ground. Our study provides important information about the mechanisms underlying the environmental adaptation and tenacious vitality of highly drug-resistant pathogens. Additionally, this study provides new insights into the prevention of infection or potential therapeutic strategies for astronauts.

Acknowledgements

This study was supported by the National Basic Research Programs of China (2014CB744400), the China Postdoctoral Science Foundation (2016M592928), the National Natural Science Foundation of China (81600011), and the National significant Science Foundation (2015ZX09J15102-003).

Disclosure of conflict of interest

None.

Address correspondence to: Changting Liu, Nanlou Respiratory Diseases Department, Chinese PLA General Hospital, Beijing 100853, China. Tel: +86-010-66876272; Fax: +86-010-66876272; E-mail: liuchangting1029@sina.com

References

[1] Su L, Chang D and Liu C. The development of space microbiology in the future: the value and significance of space microbiology research. Future Microbiol 2013; 8: 5-8.

[2] Tixador R, Richoilley G, Gasset G, Templier J, Bes JC, Moatti N and Lapchine L. Study of minimal inhibitory concentration of antibiotics on bacteria cultivated in vitro in space (Cytos 2 experiment). Aviat Space Environ Med 1985; 56: 748-751.

[3] Lapchine L, Moatti N, Gasset G, Richoilley G, Templier J and Tixador R. Antibiotic activity in space. Drugs Exp Clin Res 1986; 12: 933-938.

[4] Juergensmeyer MA, Juergensmeyer EA and Guikema JA. Long-term exposure to spaceflight conditions affects bacterial response to antibiotics. Microgravity Sci Technol 1999; 12: 41-47.

[5] Guo Y, Li Y, Su L, Chang D, Liu W, Wang T, Yuan Y, Fang X, Wang J, Li T, Fang C, Dai W and Liu C. Comparative genomic analysis of Klebsiella pneumonia (LCT-KP214) and a mutant strain (LCT-KP289) obtained after spaceflight. BMC Genomics 2014; 15: 589.

[6] Su LX, Zhou LS, Liu JW, Cen Z, Wu CY, Wang T, Zhou T, Chang D, Guo YH, Fang XQ, Wang JF, Li TZ, Yin SJ, Dai WK, Zhou YP, Zhao J, Fang CX, Yang RF and Liu CT. Phenotypic, genomic, transcriptomic and proteomic changes in Bacillus cereus after a short-term space flight. Adv Space Res 2014; 53: 18-29.

[7] Li J, Liu F, Wang Q, Ge P, Woo PC, Yan J, Zhao Y, Gao GF, Liu CH and Liu C. Genomic and transcriptomic analysis of NDM-1 Klebsiella pneumoniae in spaceflight reveal mechanisms underlying environmental adaptability. Sci Rep 2014; 4: 6216.

[8] Benoit MR, Li W, Stodieck LS, Lam KS, Winther CL, Roane TM and Klaus DM. Microbial antibiotic production aboard the International Space Station. Appl Microbiol Biotechnol 2006; 70: 403-411.

[9] Klaus D, Simske S, Todd P and Stodieck L. Investigation of space flight effects on Escherichia coli and a proposed model of underlying physical mechanisms. Microbiology 1997; 143: 449-455.

[10] Mennigmann HD and Lange M. Growth and differentiation of bacillus subtilis under microgravity. Naturwissenschaften 1986; 73: 415-417.

[11] Huang B, Liu N, Rong X, Ruan J and Huang Y. Effects of simulated microgravity and spaceflight on morphological differentiation and secondary metabolism of Streptomyces coelicolor A3(2). Appl Microbiol Biotechnol 2015; 99: 4409-4422.

[12] Guo J, Han N, Zhang Y, Wang H, Zhang X, Su L, Liu C, Li J, Chen C and Liu C. Use of genome sequencing to assess nucleotide structure variation of Staphylococcus aureus strains cultured in spaceflight on Shenzhou-X, under simulated microgravity and on the ground. Microbiol Res 2015; 170: 61-68.

[13] Wang YJ, Yuan YT, Liu JW, Su LX, Chang D, Guo YH, Chen ZH, Fang XQ, Wang JF, Li TZ, Zhou LS, Fang CX, Yang RF and Liu CT. Transcriptomic and proteomic responses of Serratia marcescens to spaceflight conditions involve large-scale changes in metabolic pathways. Adv Space Res 2014; 53: 1108-1117.

[14] Chang D, Zhu Y, An L, Liu J, Su L, Guo Y, Chen Z, Wang Y, Wang L, Wang J, Li T, Fang X, Fang C, Yang R and Liu C. A multi-omic analysis of an Enterococcus faecium mutant reveals specific genetic mutations and dramatic changes in mRNA and protein expression. BMC Microbiol 2013; 13: 304.

[15] Zhang X, Fang X and Liu C. Genomic and proteomic analysis of escherichia coli after spaceflight reveals changes involving metabolic pathways. Arch Med Res 2015; 46: 181-185.

[16] Liu C. The theory and application of space microbiology: China's experiences in space experiments and beyond. Environ Microbiol 2017; 19: 426-433.

[17] Tzouvelekis LS, Markogiannakis A, Psichogiou M, Tassios PT and Daikos GL. Carbapenemases in Klebsiella pneumoniae and other Enterobacteriaceae: an evolving crisis of global dimensions. Clin Microbiol Rev 2012; 25: 682-707.

[18] Deshpande LM, Rhomberg PR, Sader HS and Jones RN. Emergence of serine carbapenemases (KPC and SME) among clinical strains of Enterobacteriaceae isolated in the United States Medical Centers: report from the MYSTIC Program (1999-2005). Diagn Microbiol Infect Dis 2006; 56: 367-372.

[19] Nordmann P, Cuzon G and Naas T. The real threat of Klebsiella pneumoniae carbapenemase-producing bacteria. Lancet Infect Dis 2009; 9: 228-236.

[20] Mathers AJ, Peirano G and Pitout JD. The role of epidemic resistance plasmids and international high-risk clones in the spread of multidrug-resistant Enterobacteriaceae. Clin Microbiol Rev 2015; 28: 565-591.

[21] Li R, Yu C, Li Y, Lam TW, Yiu SM, Kristiansen K and Wang J. SOAP2: an improved ultrafast tool for short read alignment. Bioinformatics 2009; 25: 1966-1967.

[22] Li R, Li Y, Fang X, Yang H, Wang J, Kristiansen K and Wang J. SNP detection for massively parallel whole-genome resequencing. Genome Res 2009; 19: 1124-1132.

[23] Langmead B and Salzberg SL. Fast gapped-read alignment with Bowtie 2. Nat Methods 2012; 9: 357-359.

[24] Trapnell C, Roberts A, Goff L, Pertea G, Kim D, Kelley DR, Pimentel H, Salzberg SL, Rinn JL and Pachter L. Differential gene and transcript expression analysis of RNA-seq experiments with TopHat and cufflinks. Nat Protoc 2012; 7: 562-578.

[25] Mortazavi A, Williams BA, McCue K, Schaeffer L and Wold B. Mapping and quantifying mammalian transcriptomes by RNA-Seq. Nat Methods 2008; 5: 621-628.

[26] Lee KW, Periasamy S, Mukherjee M, Xie C, Kjelleberg S and Rice SA. Biofilm development and enhanced stress resistance of a model, mixed-species community biofilm. ISME J 2014; 8: 894-907.

[27] Andrade LN, Vitali L, Gaspar GG, Bellissimo-Rodrigues F, Martinez R and Darini AL. Expansion and evolution of a virulent, extensively drug-resistant (polymyxin B-resistant), QnrS1-, CTX-M-2-, and KPC-2-producing Klebsiella pneumoniae ST11 international high-risk clone. J Clin Microbiol 2014; 52: 2530-2535.

[28] Harms A, Maisonneuve E and Gerdes K. Mechanisms of bacterial persistence during stress and antibiotic exposure. Science 2016; 354: 4268.

[29] Zea L, Prasad N, Levy SE, Stodieck L, Jones A, Shrestha S and Klaus D. A molecular genetic basis explaining altered bacterial behavior in space. PLoS One 2016; 11: e0164359.

[30] Leonardi R and Roach PL. Thiamine biosynthesis in Escherichia coli: in vitro reconstitution of the thiazole synthase activity. J Biol Chem 2004; 279: 17054-17062.

[31] Gigliobianco T, Lakaye B, Wins P, El Moualij B, Zorzi W and Bettendorff L. Adenosine thiamine triphosphate accumulates in Escherichia coli cells in response to specific conditions of metabolic stress. BMC Microbiol 2010; 10: 148.

[32] Sleator RD and Hill C. Bacterial osmoadaptation: the role of osmolytes in bacterial stress and virulence. FEMS Microbiol Rev 2002; 26: 49-71.